Pergamon

Tetrahedron: *Asymmetry* 10 (1999) 4695–4700

TETRAHEDRON:
ASYMMETRY

Synthesis of a novel cage-functionalized chiral binaphthol host: a potential new agent for enantioselective recognition of chiral ammonium salts

Alan P. Marchand,* Hyun-Soon Chong and Bishwajit Ganguly

Department of Chemistry, University of North Texas, Denton, Texas 76203-5070, USA

Received 9 October 1999; accepted 12 November 1999

Abstract

Optically active, cage-functionalized crown ether (*R*)-**3** which contains a 1,1′-bi-2-naphthol moiety has been prepared. Subsequently, the ability of (*R*)-**3** to selectively recognize the enantiomers of guest ammonium salts, i.e., **4** and **5** in transport experiments was studied. Host (*R*)-**3** displays significantly enhanced enantiomeric selectivity toward complex formation with **4** vis-à-vis complex formation with **5**. The relative energetics of various relevant host–guest complexes have been investigated computationally.

1. Introduction

A variety of optically active macrocyclic crown ethers[1] that serve as 'host' systems that are capable of differentiating between enantiomeric 'guest' molecules during host–guest complexation have been prepared via incorporation of chiral elements into the crown ring skeleton. In particular, chiral recognition of racemic primary amines by crown ethers that contain one or more 1,1′-bi-2-naphthol moieties has received special attention.[2] Although a large number of these binaphthol-containing crown ethers have been prepared, to the best of our knowledge no examples of a cage-annulated system hitherto have been reported.

In previous studies of cage-functionalized crown ethers and cryptands, we have demonstrated that incorporation of a cage moiety into the host system can have a dramatic effect upon the ability of the host molecule: (i) to form complexes with, e.g., alkali metal cations; and (ii) to transport species of this type through a liquid membrane.[3] As a part of our continuing interests in 'host–guest chemistry',[4] we now report the synthesis of (*R*)-**3** (Scheme 1), an optically active, cage-functionalized crown ether in which a 1,1′-bi-2-naphthol moiety has been incorporated as the source of chirality. The ability of (*R*)-**3** to

* Corresponding author. E-mail: marchand@unt.edu

0957-4166/99/$ - see front matter
PII: S0957-4166(99)00549-2

demonstrate enantiomeric recognition during complexation of chiral ammonium ions has been evaluated as part of this study.

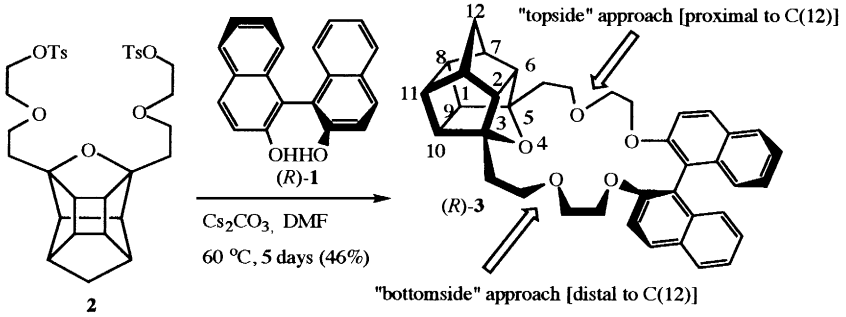

Scheme 1.

2. Results and discussion

2.1. Synthesis and ammonium ion transport experiments

Axially dissymmetric 1,1′-bi-2-naphthol (*R*)-**1** was used as the chiral component to prepare (*R*)-**3**. Thus, Cs^+-templated reaction of **2** with (*R*)-**1** produced (*R*)-**3** in 46% yield (Scheme 1). The structure of (*R*)-**3** was confirmed via analysis of its respective ^{1}H NMR and ^{13}C NMR spectra and via HRMS analysis (see Experimental). The maximum value of the optical rotation for (*R*)-**3** was determined by polarimetry to be $[\alpha]_D$=+54.0 (*c* 0.2, $CHCl_3$).

It is interesting to note that whereas the starting material, i.e. **2**,[4] is achiral (*meso*), this symmetry element is lost when **2** is converted into (*R*)-**3**. In addition, host molecule (*R*)-**3** presents two potential complexation 'faces' to an approaching guest molecule. Thus, as host–guest complex formation progresses, the guest molecule can pursue either a 'topside' approach to (*R*)-**3**, i.e., along a trajectory proximal to C(12) in the 4-oxahexacyclo[5.4.1.0^{2,6}.0^{3,10}.0^{5,9}.0^{8,11}]dodecyl cage moiety, or a 'bottomside' approach to (*R*)-**3** in which the approaching guest follows a trajectory that lies distal to the C(12) carbon atom in this moiety (see Scheme 1).

Next, the ability of (*R*)-**3** to discriminate between transport of enantiomeric 'guests', i.e., (±)-α-methylbenzylethylammonium chloride (**4**) and methyl (±)-phenylglycinate hydrochloride (**5**), through a liquid ($CHCl_3$) membrane was explored by means of a simple U-tube experiment.[5] The results thereby obtained are shown in Table 1. Examination of the data in Table 1 indicates that (*R*)-**3** displays significantly higher enantiomeric selectivity toward complexation and transport of **4** vis-à-vis **5**. Thus, during a contact time of 4 h, (*R*)-**3** transported (10±2)% of **4** with (79±10)% enantiopurity by complexing preferentially with (*S*)-**4**. By way of contrast, (*R*)-**3** displays relatively low enantiomeric recognition toward **5**. During the same contact time (4 h) the chiral host transported (12±3)% of **5** through the $CHCl_3$ membrane with only (15±4)% enantiopurity by complexing preferentially with (*R*)-**5**. In control studies (Table 1, run numbers 2 and 4), the host ligand was not present in the $CHCl_3$ layers, and a longer contact time (24 h) was employed. Under these conditions, only ca. 3% of (racemic) guest was transported through the $CHCl_3$ membrane.

Table 1
Differential transport (U-tube experiment) of enantiomers of **4** and **5** by 0.027 M host (*R*)-**3** in $CHCl_3$

run no.	time (h)	host	guest	% transferred	configuration of dominant enantiomer	enantio-purity (%)
1	4	(*R*)-**3**	**4**[b]	9.7 ± 2.0	*S*	78.7 ± 9.5
2	24	none	**4**[b]	3.2 ± 0.5		
3	4	(*R*)-**3**	**5**[c]	12.1 ± 3.2	*R*	14.7 ± 3.5
4	24	none	**5**[c]	3.3 ± 1.5		

[a]Averages and standard deviations calculated for data obtained from three independent transport experiments; [b](±)-α-methylbenzylammonium chloride; [c]methyl (±)-phenylglycinate hydrochloride

2.2. *Results of molecular mechanics calculations*[6]

As complex formation between (*R*)-**3** with **4** or **5** progresses, the RNH_3^+ group in the guest molecules enters into hydrogen bonding with various donor atoms of the host molecule. In order to assess the extent to which complex formation occurs and also to identify the preferred binding sites in each case, we have performed molecular mechanics calculations by using MacroModel (v. 5.0)[7] to perform Monte Carlo conformational searches (1000 structures). The complexes were generated by manual docking of the guests into the cavity of hosts by using MacroModel.[6] The geometries of the resulting complexes were optimized by employing the PRCG algothrim with the Amber* force field and the GB/SA solvation model for H_2O.[8] In this way, the propensity of individual enantiomers of **4** and **5**, respectively, to bind to (*R*)-**3** via 'topside' vs 'bottomside' approaches to the optically active host molecule has been investigated.

The geometric features of the calculated complexes suggest that host–guest hydrogen bonding indeed plays an important role. In each case, the RNH_3^+ group in the guest molecule fits snugly into the macrocyclic cavity of the host, and the resulting complex receives extensive stabilization via efficient $RH_2N^+H\cdots O$ hydrogen bond formation. The relative binding energies for these complexes, shown in Table 2, predict that complex formation that results via 'topside' approach of the guest upon the host is preferred vis-à-vis the alternative mode of complex formation that would result via the corresponding 'bottomside' approach by individual enantiomers of **4**. Thus, (*S*)-**4** is predicted to bind preferentially (by ca. 1.3 kcal mol^{-1}) to the 'topside' face of (*R*)-**3**.

Interestingly, there appears to be little preference for binding of (*R*)-**3** to either (*R*)-**5** or (*S*)-**5**. Here, binding of the (*R*)-**5** enantiomer to the 'topside' face of (*R*)-**3** is marginally preferred (see results of calculations that appear in Table 2).

Herein, we observed that (*R*)-**3** appears to bind with high enantioselectivity to (*S*)-**4** but with only modest enantioselectivity to (*R*)-**5**. The results of molecular mechanics calculations provide insight into possible reasons for this behavior by revealing a fundamental difference between the relative orientations of these two guest ammonium ions in their respective energy minimized 1:1 host–guest complexes with (*R*)-**3**. Thus, the preferred mode of 'topface' binding of (*S*)-**4** to (*R*)-**3** results in alignment of the carbon–phenyl bond in the guest with the major axis of the optically active host (see Fig. 1A). However, the corresponding energy minimized structure of the relevant 1:1 host–guest complex of (*R*)-**5** with (*R*)-**3** indicates that 'topface' binding results in alignment of the carbon–phenyl bond in the guest with the minor axis of the host (see Fig. 1B). It thus appears that increased host–guest interactions are possible

Table 2
Calculated (Amber*) relative complexation energies (kcal mol^{-1}) of (*R*)-**3** to (*R*)-**4**, (*S*)-**4**, (*R*)-**5**, and (*S*)-**5**, respectively

Host-Guest Complex	**"topside" face**		**"bottomside" face**	
(*R*)-**3** (host) + **4** (guest)	(*R*)-**3** + (*R*)-**4**	(*R*)-**3** + (*S*)-**4**	(*R*)-**3** + (*R*)-**4**	(*R*)-**3** + (*S*)-**4**
	1.3	0.0	2.8	2.0
(*R*)-**3** (host) + **5** (guest)	(*R*)-**3** + (*R*)-**5**	(*R*)-**3** + (*S*)-**5**	(*R*)-**3** + (*R*)-**5**	(*R*)-**3** + (*S*)-**5**
	0.0	0.5	0.3	1.1

in the former orientation which more closely juxtaposes the bulky aryl groups of the host and guest in the complex, with the result that increased enantiodiscrimination is possible in the (*R*)-**3**–(*S*)-**4** complex vis-à-vis the corresponding (*R*)-**3**–(*R*)-**5** complex.

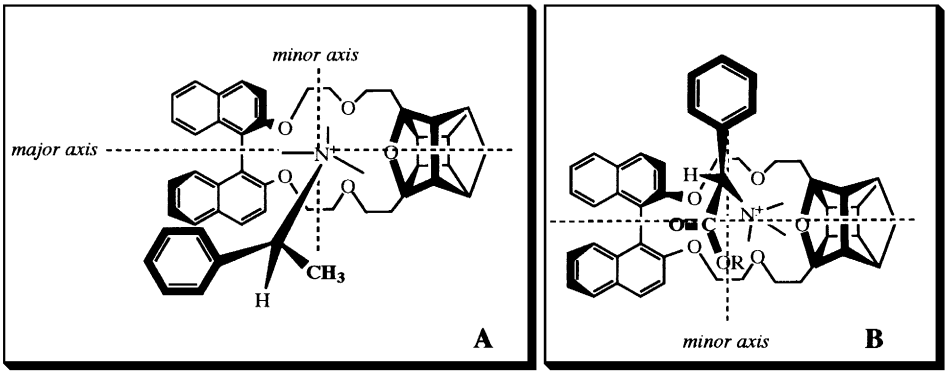

Fig. 1. A. Energy minimized 1:1 host–guest complex between (*R*)-**3** and (*S*)-**4**. B. Energy minimized 1:1 host–guest complex between (*R*)-**3** and (*R*)-**5**

3. Conclusions

Cage-functionalized optically active crown ether (*R*)-**3** has been prepared into which a 1,1′-bi-2-napthol moiety has been incorporated as the source of chirality. The ability of (*R*)-**3** to bind enantioselectively to guest ammonium salts **4** and **5** has been assessed by means of a simple U-tube (transport) experiment. The results thereby obtained (Table 1) suggest that (*R*)-**3** binds to (*S*)-**4** with high enantioselectivity, but this optically active host binds to (*R*)-**5** with only modest enantioselectivity.

The results of molecular mechanics calculations shown in Table 2 agree qualitatively with our experimental observations. In addition, the relative binding energies obtained via molecular mechanics calculations predict that binding of the RNH_3^+ group in the guest molecule occurs preferentially through the ‘topside’ face of the host.

4. Experimental

4.1. General

Melting points are uncorrected. All UV readings were recorded by using a Hewlett–Packard Model 84524 Diode Array UV–vis spectrophotometer. Optical rotations were taken on a Perkin–Elmer 241 polarimeter. High-resolution mass spectral data reported herein were obtained by Professor Jennifer S. Brodbelt at the Mass Spectrometry Facility at the Department of Chemistry and Biochemistry, University of Texas at Austin by using a ZAB-E double sector high-resolution mass spectrometer (Micromass, Manchester, England) that was operated in the chemical ionization mode. Host ligand that possessed maximum optical rotation was used unless otherwise noted. Prior to reuse, the host was purified by chromatography to remove small amounts of accrued oxidation products. Spectroscopic grade $CHCl_3$ was washed with water to remove EtOH.

4.2. Cage-functionalized chiral crown ether (R)-3

A solution of **1** (124 mg, 0.43 mmol) and **2** (273 mg, 0.42 mmol) in DMF (13 mL) was added dropwise to a stirred suspension of Cs_2CO_3 (291 mg, 0.89 mmol) in DMF (51 mL) at 60°C during 5 h. The reaction mixture then was filtered, and the filtrate was concentrated in vacuo. The residue was dissolved in CH_2Cl_2 (20 mL) and washed sequentially with water (2×20 mL) and 2N aqueous NaOH (2×20 mL). The organic layer was dried ($MgSO_4$) and filtered, and the filtrate was concentrated in vacuo. The residue was purified via column chromatography on silica gel by eluting with 15% EtOAc–hexane. Pure (*R*)-**3** was thereby obtained as a colorless viscous oil (124 mg, 49%: $[\alpha]_D$=+54.0 (*c* 0.2, $CHCl_3$); ^{1}H NMR ($CDCl_3$) δ 1.47 (*A*B, J_{AB}=9.8 Hz, 1H), 1.79–1.93 (m, 5H), 2.21–2.60 (m, 8H), 3.23–3.50 (m, 8H), 3.95–4.18 (m, 4H), 7.10–7.36 (m, 6H), 7.46 (d, *J*=9.1 Hz, 2H), 7.87 (d, *J*=8.0 Hz, 2H), 7.94 (d, *J*=9.1 Hz, 2H); ^{13}C NMR ($CDCl_3$) δ 32.4 (t), 41.8 (d, 2C), 43.2 (t, 2C), 44.3 (d, 2C), 48.27 (d), 48.33 (d), 58.72 (d), 58.77 (d), 68.11 (t), 68.14 (t), 69.80 (t), 69.84 (t), 69.9 (t, 2C), 94.2 (s, 2C), 117.00 (d), 117.03 (d), 120.0 (s), 120.3 (s), 123.1 (d, 2C), 124.0 (d, 2C), 125.8 (d, 2C), 126.4 (d, 2C), 129.50 (d), 129.52 (d), 130.1 (s, 2C), 134.32 (s), 134.35 (s), 154.35 (s), 154.37 (s). Exact mass (CI HRMS) calcd for $C_{39}H_{38}O_5$: M_r^+ *m/z* 587.27975. Found: M_r^+ *m/z* 587.27628.

4.3. U-Tube transport experiments

Cation transport experiments were performed in a simple U-tube apparatus by using a previously published procedure.[5] Thus, in a 14 mm i.d. U-tube at 24±1°C was placed a 0.027 M solution of optically active (*R*)-**3** in $CHCl_3$ (10 mL, 0.27 mmol). Into the α-arm of the U-tube (source phase) was introduced 5.0 mL of a solution that contained 1.0 mmol of the guest ammonium salt (i.e., racemic **4** or **5**) and was 0.08 M in aqueous HCl and 0.8 M in $LiPF_6$. Into the β-arm of the U-tube (receiving phase) was placed 0.10 M aqueous HCl (5.0 mL, 0.50 mmol). A small magnetic stirring bar was used to mix the aqueous and $CHCl_3$ layers at a constant rate. The absorbance of the aqueous receiving phase (β-arm) in the UV spectrum was measured at λ=256 nm for **4** and at λ=272 nm for **5**. The presence of host (*R*)-**3** could not be detected in the UV spectrum of the receiving phase (β-arm). At the conclusion of the transport experiment, the aqueous solution in the receiving phase (β-arm) was removed via pipet, and the β-arm was washed with water (5 mL). To the combined aqueous solutions was added dropwise 3% aqueous NH_4OH with stirring until the solution had become basic to litmus. The resulting aqueous suspension was extracted with CH_2Cl_2 (2×10 mL). The organic extracts were dried ($MgSO_4$) and filtered, and the

filtrate was concentrated in vacuo. The residue thereby obtained was diluted with CH_2Cl_2 to a total volume of 1 mL. The resulting solution was placed in a 1 mL polarimetry cell, and its optical rotation was determined.[5]

Acknowledgements

We thank the United States Department of Energy (grant DE-FG07-98ER14936) and the Robert A. Welch Foundation (grant B-963) for financial support of this study. In addition, we thank Professor Jennifer S. Brodbelt (Department of Chemistry, University of Texas at Austin) for having kindly obtained high-resolution chemical ionization mass spectral data for (*R*)-**3**.

References

1. (a) Cram, J. M. *Science* **1988**, *240*, 760. (b) Konishi, K.; Yahara, K.; Toshishige, H.; Aida, T.; Inoue, S. *J. Am. Chem. Soc.* **1994**, *116*, 1337. (c) Izatt, R. M.; Wang, T. M.; Huszthy, P.; Zhu, C. Y.; Bradshaw, J. S. *J. Inclusion Phenom. Mol. Recogn. Chem.* **1994**, *18*, 353. (d) Yamamoto, K.; Yumioka, H.; Okamoto, Y.; Chikamatsu, H. *J. Chem. Soc., Chem. Commun.* **1987**, 168.
2. (a) Kyba, E. P.; Koga, K.; Sousa, L. R.; Siegel, M. G.; Cram, D. J. *J. Am. Chem. Soc.* **1973**, *95*, 2692. (b) Cram, J. M. *Science* **1974**, *183*, 803. (c) Kyba, E. P.; Timko, J. M.; Kaplan, L. J.; de Jong, F.; Gokel, G. W.; Cram, D. J. *J. Am. Chem. Soc.* **1978**, *100*, 4555. (d) Sogah, G. D. Y.; Cram, D. J. *J. Am. Chem. Soc.* **1979**, *101*, 3035. (e) Galán, A.; Andreu, D.; Echavarren, A. M.; Prados, P.; de Mendoza, J. *J. Am. Chem. Soc.* **1992**, *114*, 1511. (d) Yamamoto, K.; Yumioka, H.; Okamoto, Y.; Chikamatsu, H. *J. Chem. Soc., Chem. Commun.* **1987**, 168.
3. (a) Marchand, A. P.; Kumar, K. A.; McKim, A. S.; Mlinaric-Majerski, K.; Kragol, G. *Tetrahedron* **1997**, *53*, 3467. (b) Marchand, A. P.; Alihodzic, S.; McKim, A. S.; Kumar, K. A.; Mlinaric-Majerski, K.; Kragol, G. *Tetrahedron Lett.* **1998**, *39*, 1861.
4. (a) Marchand, A. P.; Chong, H.-S.; Alihodzic, S.; Watson, W. H.; Bodige, S. G. *Tetrahedron* **1999**, *55*, 9687. (b) Marchand, A. P.; Chong, H.-S. *Tetrahedron* **1999**, *55*, 9697.
5. Newcomb, M.; Toner, J. L.; Helgeson, R. C.; Cram, D. J. *J. Am. Chem. Soc*. **1979**, *101*, 4941.
6. Molecular mechanics calculations have been utilized extensively to provide insight into the factors that influence enantioselectivity in host–guest complexation. For recent examples in this regard, see: (a) Asakawa, M.; Brown, C. L.; Pasini, D.; Stoddart, J. F.; Wyatt, P. G. *J. Org. Chem.* **1996**, *61*, 7234. (b) Garcia, C.; Guyor, J.; Jeminet, G.; Leize-Wagner, E.; Nierengarten, H.; Van Dorsselaer, A. *Tetrahedron Lett.* **1999**, *40*, 4997.
7. Mohamadi, F.; Richards, N. G. J.; Guida, W. C.; Liskamp, R.; Lipton, M.; Caufield, C.; Chang, G.; Hendrickson, T.; Still, W. C. *J. Comput. Chem.* **1990**, *11*, 440.
8. Still, W. C.; Tempczyk, A.; Hawley, R. C.; Hendrickson, T. *J. Am. Chem. Soc*. **1990**, *112*, 6127.